Civil Engineering Beyond Limits 3 (2024) 1964

Civil Engineering Beyond Limits

journal home: www.acapublishing.com/journals/1/cebel

Research Article

Seismic Evaluation of RC Building Designed by 1975 Turkish Seismic Code (A Case Study)

Mustafa Kırat,[1] , Mehmet Fatih Yılmaz*,[2]

[1] *Civil Engineer, Bank of Provinces,Samsun,Turkey*

[2] *Ondokuz Mayıs University,Engineering Faculty,Department of Civil Engineering,Samsun,Turkey*

Keywords

Seismic performance,
Nonlinear analysis,
Confined concrete,
Damage states,
Plastic hinge formation,
Stirrup configuration,
Pushover analysis.

Abstract

This study evaluates the seismic performance of a five-story reinforced concrete building located in Samsun, designed according to the 1975 Earthquake Code, using the principles of TBDY 2018. The structure was modeled using the ETABS analysis program, and an incremental pushover analysis was applied. The effects of different stirrup arrangements and hook angles on structural performance were investigated. The analysis results indicate that confining the end regions of columns and using 135° hook angles significantly improved the damage levels of the columns. Model D demonstrated the best performance, minimizing plastic hinge formation and achieving the highest ductility at target displacement levels. In contrast, Model A, which lacked confinement and used 90° hooks, exhibited weaker performance. The target displacement values were determined as 57.286 mm in the X-direction and 30.838 mm in the Y-direction. The obtained capacity curves and plastic hinge distributions clearly illustrate the seismic performance of the building under various scenarios. The results emphasize the critical importance of adhering to design principles specified in earthquake codes to ensure structural resilience. Additionally, it was observed that the building, constructed in 1995 based on the 1975 Earthquake Code, did not exhibit collapse or advanced damage levels when analyzed under TBDY 2018 standards. This highlights the necessity of accurately defining material properties and detailing in compliance with regulatory requirements during the design phase to ensure seismic resilience. Future studies can focus on time-history analyses, the effects of material variations, and retrofitting techniques for older structures to further deepen the findings.

1. Introduction

Earthquakes are natural phenomena that occur as a result of the sudden release of energy accumulated in the Earth's crust and are often associated with destructive effects Kanamori and Brodsky (2004) [12]. The seismic waves generated during this energy release impose recurring and dynamic loads on structures, creating impacts in both vertical and horizontal planes. The magnitude, frequency, and duration of these loads are critical determinants of a structure's resilience. Factors such as inadequate engineering practices, poor material quality, and design errors can lead to severe structural damage or even complete collapse under seismic effects. Turkey, due to its active tectonic structure, is among the countries with the highest earthquake risk globally Bozkurt (2001)[13]. A significant portion of the country lies in a region where the Eurasian, Arabian, and African plates converge, intensifying seismic activity Barka and Kadinsky-Cade (1988)[14]. The two main fault lines in Turkey, the North Anatolian Fault (NAF) and the East Anatolian Fault (EAF), have been responsible for the country's most active and destructive earthquakes. Major earthquakes in Turkey, both in historical and modern times, have had significant impacts on human life and structures.

Among the notable earthquakes, the first chronologically is the 1939 Erzincan Earthquake. With a magnitude of 7.9, this earthquake resulted in the loss of over 30,000 lives and caused widespread destruction. Following this, the 1999 Marmara Earthquake occurred. Measuring 7.4 in magnitude, it deeply affected the Marmara Region, Turkey's industrial hub, claiming more than 17,000 lives and destroying thousands of buildings. This earthquake exposed significant deficiencies in structural design and construction quality. Most recently, the 2023 Kahramanmaraş Earthquakes struck. Two major earthquakes, with magnitudes of 7.7 and 7.6, caused extensive devastation in the Southeastern Anatolia Region, leading to the loss of over 50,000 lives and leaving millions homeless. These earthquakes once again highlighted the inadequacy of earthquake safety measures in structures. Earthquake codes established to ensure the construction of earthquake-resistant structures must be periodically revised, as they often fail to meet evolving requirements over time. Over the years, Turkey has continually updated its earthquake codes to enhance seismic safety, reflecting advancements in engineering and lessons learned from past events. These codes, issued chronologically, include the Italian Building Code for Construction in Earthquake Zones (1940), the Temporary Building Code for Earthquake Zones (1944), and the Building Code for Turkey's Earthquake Zones (1949). Subsequent updates include the Code on Buildings in Earthquake Zones (1953), the Code on Buildings in Disaster Areas (ABYYHY) in 1962, 1968, 1975, and 1998, the Code on Buildings in Earthquake Zones (DBYBHY) (2007), and most recently, the Turkey Building Earthquake Code (TBDY) (2018). This progression highlights the country's ongoing commitment to improving structural safety in response to evolving needs and scientific advancements.

To better understand earthquake codes, numerous studies have been conducted in the literature. In one study, two different school buildings in Adana were modelled based on their physical conditions, and their performance under various seismic levels was analyzed according to current standards Yüzbaşı et al. (2018)[5]. Similarly, another study compared the 2007 Earthquake Code (TDY 2007) and the 2018 Turkey Building Earthquake Code (TBDY 2018) by analyzing models with different structural systems and numerically comparing the results Döndüren et al. (2021)[6]. In the study titled "The Effect of Confined Concrete Behavior on the Behavior of Reinforced Concrete Elements and Systems" prepared by Özmen et al.(2007)[15], material models used in modeling the nonlinear behavior of reinforced concrete elements were examined. Within the scope of the study, the nonlinear behavior of reinforced concrete columns and beams was

*Corresponding Author: mehmetfatih.yilmaz@omu.edu.tr
Received 08 Dec 2024; Revised 18 Dec 2024; Accepted 18 Dec 2024
https://doi.org/10.36937/cebel.2024.1964

analyzed using the Mander, Modified Kent-Park, and Saatcioglu-Razvi concrete models. Analyses were conducted considering the effects of different concrete classes and confinement reinforcement spacings. The moment-curvature relationships and plastic hinge behaviors of reinforced concrete elements were evaluated. A four-story reinforced concrete structure was modeled using the SAP2000 program and subjected to a nonlinear static pushover analysis. The results showed that while concrete class and confinement reinforcement significantly affected the curvature behavior of column and beam elements, these differences had a limited impact on the overall system-level behavior. The Mander model demonstrated better performance at high curvature values, whereas the Saatcioglu-Razvi model produced results comparable to the Mander and Modified Kent-Park models, depending on concrete quality. This study highlights the importance of material models in simulating the nonlinear behavior of reinforced concrete structures and emphasizes the effectiveness of confined concrete models in ensuring seismic safety. In the study titled "Pushover and Nonlinear Time History Analysis Evaluation of a RC Building Collapsed During the Van (Turkey) Earthquake on October 23, 2011" by Çavdar and Bayraktar (2014)[16], the seismic performance of a six-story reinforced concrete building that collapsed during the 2011 Van earthquake was evaluated using static pushover analysis and nonlinear time history analysis methods. The building was designed according to the 1975 Earthquake Code, but its performance analysis was conducted based on the standards of the 2007 Earthquake Code. The building was modeled in SAP2000, utilizing user-defined plastic hinge properties for the analysis. The static pushover analysis results indicated that the building was at the "pre-collapse" performance level and could not meet the demands under the design earthquake. Nonlinear time history analysis results revealed a collapse mechanism concentrated on the lower floors due to the formation of plastic hinges primarily in the first two stories. Moreover, significant differences were observed between the results of the two analysis methods, with the time history analysis predicting higher levels of damage. The study highlighted that inadequate reinforcement detailing, poor concrete quality, and substandard workmanship severely affected the seismic performance of reinforced concrete structures. While static pushover analysis was noted as more practical, time history analysis was emphasized as providing more realistic results. In the study by Özkarabulut (2024)[17], the Mander and Köksal-Erdoğan models used for analyzing the nonlinear behavior of reinforced concrete elements were comprehensively compared. The study particularly highlighted the capacity of the Köksal-Erdoğan model to accurately represent nonlinear behaviors and demonstrated its usefulness as a tool in seismic performance analyses. The findings were evaluated to emphasize the effectiveness of nonlinear analysis methods and to support approaches used in structural performance evaluations. All these studies serve as valuable guides for understanding the regulations and seismic calculations. In this study, a building in Samsun was modeled using the ETABS analysis program, and the impact of different stirrup configurations on structural damage levels was assessed through incremental pushover analysis based on TBDY 2018.

2. General information about the building used in the model

The building modeled in this study is located in Samsun and was constructed in 1995 following the standards of the Regulation on Buildings in Disaster Areas (ABYYHY-1975). It is a five-story reinforced concrete frame structure, consisting of a basement, ground floor, and three stories with the same layout. The building has a rectangular plan width of 14.10 x 16.20 meters and is freestanding with no attached structures on any side. The story height is uniform across all floors, measuring 2.80 meters (Figure 2). The modelled building includes 13 columns and 8 shear walls distributed strategically to enhance structural stability. The slab spans in the X-direction are 390 cm, 350 cm, and 210 cm, while in the Y-direction, the spans are 655 cm, 220 cm, and 305 cm (Figure 1). These dimensions reflect the original design and structural layout of the building. The structural system is a reinforced concrete frame, comprising shear walls, columns, beams, and slab systems of various dimensions. The existing columns are rectangular in cross-section and remain consistent in dimensions throughout all floors. This uniformity ensures that the structural behavior of the columns does not vary across the height of the building, enabling a more straightforward analysis of its performance under seismic loads.

3. General information about the model

Modeling and analyses were performed using the structural analysis software ETABS V20.3.0. The Equivalent Earthquake Load Method was employed for seismic analyses. The slabs were modeled under the assumption of rigid diaphragm behavior, with the floor masses concentrated at the center of mass of each story. To determine the existing concrete strength, a total of 15 concrete core samples were taken, with three samples from the basement, ground floor, and each typical floor. Based on the test results, the existing concrete class was determined to be C21.5 MPa, with a calculated standard deviation yielding a final value of C16 MPa, which was used in the material definition for the model. Structural system elements were designed using reinforcement steel S220. Column dimensions were varied as 30x50 cm, 50x30 cm, 30x60 cm, and 60x30 cm. Beam dimensions were specified as 30x50 cm, 20x50 cm, 20x45 cm, 20x70 cm, and 30x70 cm (Figure 3). To enhance structural safety, shear wall dimensions were designed as 20x300 cm, 20x400 cm, and 20x180 cm, with the thickness of basement shear walls set at 25 cm. The slab thickness was applied as 12 cm. The material properties of C16 concrete and S220 steel used in the model are summarized in Table 1.

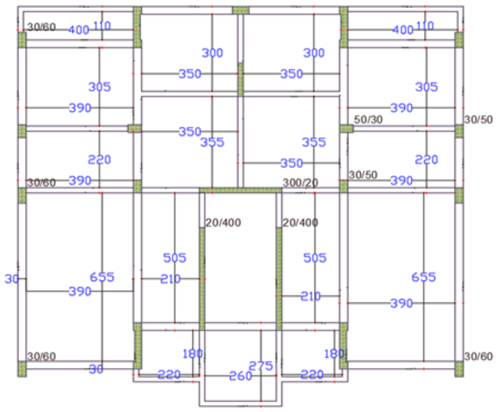

Figure 1. Belonging to the modelled structure floor plan (centimeters)

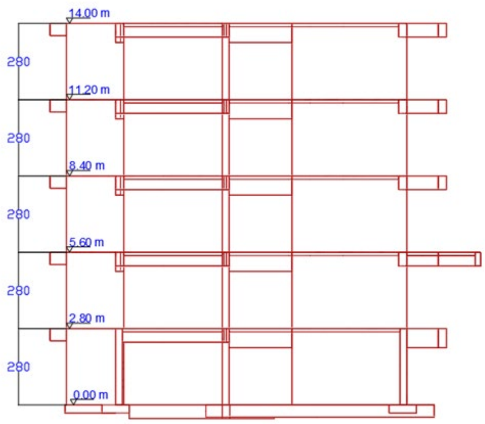

Figure 2. Belonging to the modelled structure section view

Table 1. Material properties of C16 concrete and S220 steel

Property	C16 Concrete (MPa)	S220 Steel (MPa)
Compressive Strength(f'c)	16	-
Tensile Strength(ft)	1.6	-
Modulus of Elasticity(E)	27,000 MPa	200,000 MPa
Density (ρ)	2400 kg/m³	7850 kg/m³
Yield Strength (fy)	-	220
Ultimate Strength(fu)	-	360

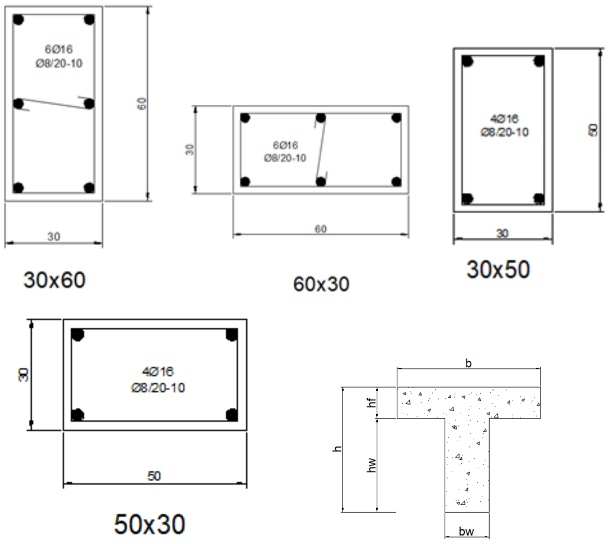

Figure 3. Details of load-bearing elements in the model

The dead and live loads affecting the models were determined in accordance with TS-498 and utilized in the calculations (Table 2).

Table 2. Loads

Load Type	Description	Values
Dead Loads	Weight of concrete, steel, and coverings	2.5 kN/m² (including coverings)
Live Loads	Load from people, furniture, and equipment	2 kN/m²
Wind Loads	Wind pressure	1.5 kN/m²
Snow Loads	Weight of snow on the roof	0.75 kN/m²

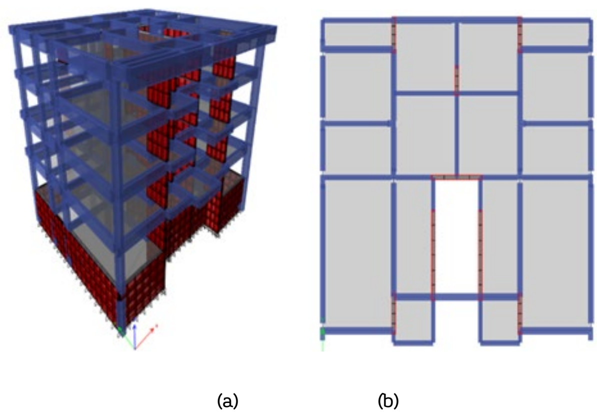

Figure 4. ETABS model a) 3d and b) floor plan views

In structural analysis using Etabs, frame finite elements and shell finite elements are widely employed to model different structural components. Frame finite elements are primarily used to represent beams and columns as linear members, efficiently capturing axial forces, bending moments, and shear forces. These elements are modelled as line segments connecting nodes, with their cross-sectional properties, such as dimensions and material characteristics, defined for accurate analysis. They are particularly effective for simulating the load-bearing behaviour of structural members and allow for the modelling of nonlinear effects like plastic hinge formation. On the other hand, shell finite elements are used to model surface elements like shear walls and slabs, which require detailed analysis of stresses and deformations across their surfaces. These elements are characterized by their thickness, material properties, and stress-strain relationships, enabling the analysis of both in-plane and out-of-plane behaviors. To enhance accuracy, shell elements are divided into smaller mesh segments, ensuring precise simulation of stress distribution. Together, these modelling techniques provide a comprehensive representation of structural components, enabling accurate assessment of their behaviour under various loading conditions.

4. Seismicity and local soil class

The design acceleration spectrum for the model created according to TBDY 2018 was calculated using the map spectral acceleration coefficients obtained from the Turkey Earthquake Hazard Maps available at https://tdth.afad.gov.tr.Forthe seismic calculation, the DD-2 (Design Basis Earthquake) earthquake ground motion, which has a 10% probability of exceedance in 50 years, was considered. For the structure located within the boundaries of Samsun province, at the coordinates of latitude 41.33 and longitude 36.285, the map spectral acceleration coefficients were determined as Ss (Short Period Spectral Acceleration Coefficient) =0.508 and S1(1-Second Period Spectral Acceleration Coefficient) =0.179 . Additionally, the soil class was defined as ZC (soil class), and based on these parameters, the design acceleration spectrum was developed (Figure 5).

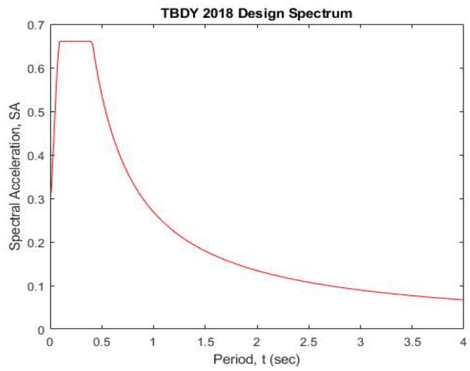

Figure 1. The earthquake design spectrum generated according to the TBDY 2018 DD-2 earthquake level

5. Determination of target displacement

The capacity curve illustrates the relationship between the lateral load applied to a structure and the displacement at its top point. This curve helps in understanding the strength and ductility characteristics of a structure. The nonlinear properties of the load-bearing elements of the model created in ETABS have been defined. These properties are crucial for understanding the performance of elements in nonlinear analyses, such as plastic hinge and fiber hinge approaches, as well as incremental pushover analysis. The plastic hinge model is a method used to simulate the nonlinear behavior exhibited by structural elements beyond their elastic limits. This approach is widely used in incremental pushover analyses and is based on the assumption that nonlinear deformations are concentrated in specific regions of the elements, typically at their ends FEMA (2000)[11]. The fiber hinge model, on the other hand, is an approach that provides a more detailed representation of material properties for structural elements in nonlinear analyses. In this model, the cross-section of an element is divided into small fibers, and the nonlinear behavior of each fiber is defined by the material's stress-strain relationship Mander et al. (1988)[12]. An incremental pushover analysis was applied to the model, and as the load increased, plastic hinges formed in the structural elements (Figure 6).

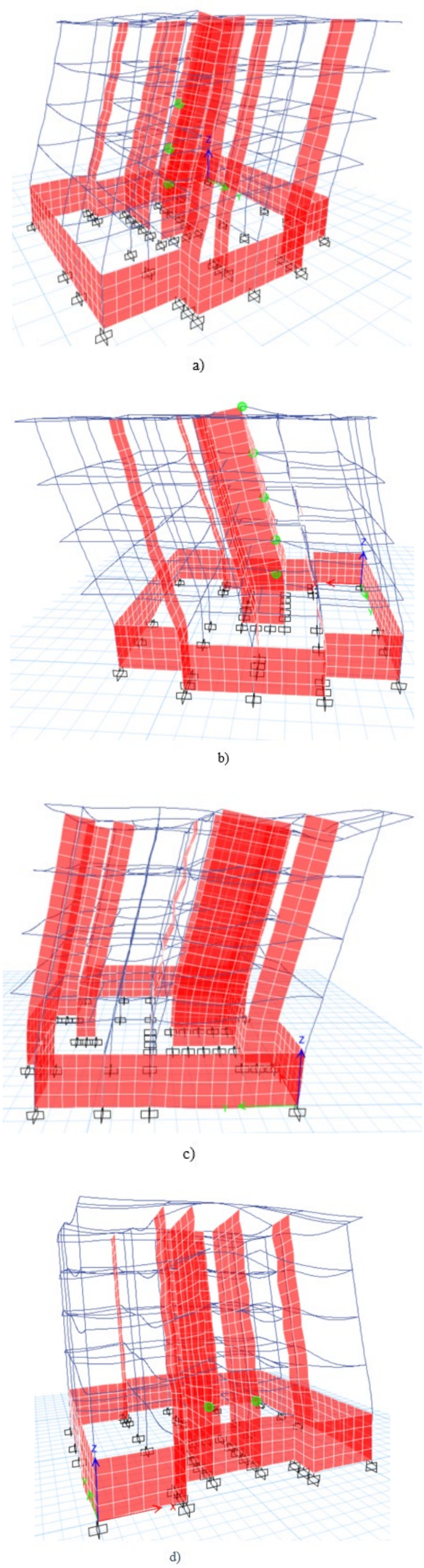

Figure 2. Plastic hinge formation a) pushxp, b) pushxn, c) pushyp and d) pushyn

Understanding the capacity spectrum and target displacement is critical, as highlighted in similar studies analyzing structural behavior under extreme loads Demirel and Polat (2020)[13]. The load and top displacement values were plotted, and the resulting capacity curves were generated as follows (Figure 7). In structural performance analyses, a specific limit value (e.g., peak displacement) is typically chosen to evaluate the building's strength and ductility against the design earthquake. A value such as 100 mm represents acceptable damage limits for the structure.

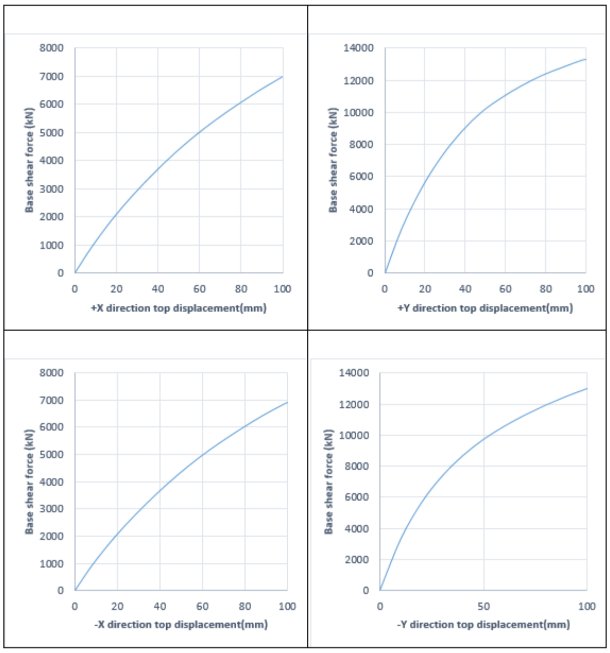

Figure 3. Capacity curves of the model

Target displacement refers to the maximum horizontal displacement expected at the top of a structure during a specified earthquake. This value is calculated using the capacity curve and the earthquake spectrum. The Capacity Spectrum Method was employed in the calculations. The capacity curve was converted into the spectral acceleration (Sa) and spectral displacement (Sd), taking into account unit weight and story masses. The acceleration-spectrum curve defined in the 2018 Earthquake Code was plotted alongside the capacity curve, and the intersection point of these curves was identified. This intersection represents the target displacement, which corresponds to the maximum horizontal displacement the structure is expected to experience during an earthquake. Based on the analysis, the target displacement was determined to be 57.286 mm in the X-direction and 30.838 mm in the Y-direction (Figure 8).

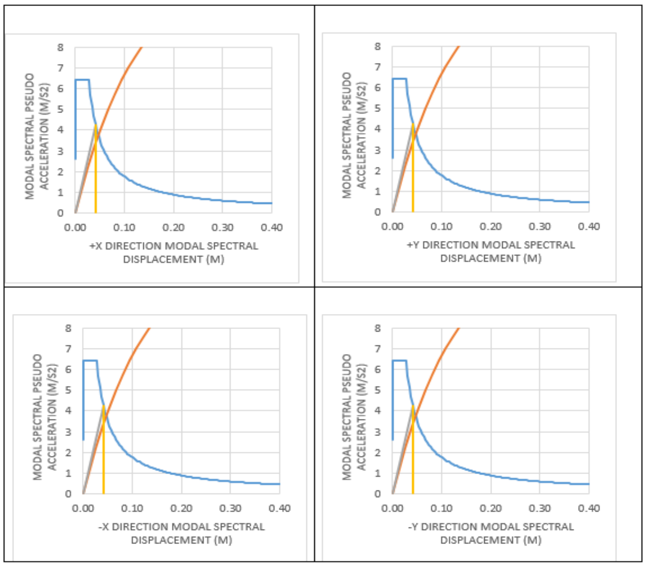

Figure 4. Determination of earthquake displacement demands

6. Development of mander material models

The Mander Material Model provides a comprehensive framework for analysing the nonlinear behaviour of reinforced concrete by distinguishing between confined and unconfined conditions. Unconfined concrete typically demonstrates brittle behaviour, with limited ductility and a rapid loss of strength following the peak stress. In contrast, confined concrete benefits from the lateral pressure applied by confinement reinforcement, such as stirrups, which enhances its compressive strength and ductility. This lateral pressure leads to a stress-strain curve with a longer plateau, indicating greater deformation capacity and improved energy dissipation under extreme loads. The model quantitatively defines the confinement effects through parameters like f'_{cc} (the maximum compressive strength of confined concrete), f'_{co} (the compressive strength of unconfined concrete), and f'_{l} (lateral pressure from confinement reinforcement). The relationship between these parameters enables an accurate representation of how confinement influences concrete performance. Additionally, the model incorporates the behaviour of reinforcement steel, capturing its elastic-plastic response and its critical role in lateral confinement. The behaviour of rebar (reinforcement steel) is also a crucial component of this model. Initially, rebar demonstrates elastic behaviour, defined by its modulus of elasticity (E_s), with a linear stress-strain relationship. Once the yield point (f_y) is reached, the steel transitions into a plastic region, allowing it to undergo significant elongation without a substantial increase in stress. This plasticity is vital for energy dissipation during seismic events. Furthermore, rebar plays a significant role in providing lateral confinement to concrete, increasing its compressive capacity and ductility. The Mander model also accounts for the longitudinal and transverse spacing of confinement bars, which directly affects the efficiency of the confinement. These features make the Mander Model an essential tool in seismic performance analyses, particularly for evaluating the behaviour of plastic hinges and the overall ductility of structural elements in seismic zones. The model's ability to realistically simulate the behaviour of both concrete and rebar under extreme loads ensures its effectiveness in non-linear static and dynamic analyses, such as pushover and time-history analyses. It is widely used in structural performance evaluations, especially for columns and beams, where accurate prediction of ductility and energy dissipation is critical Mander et al. (1988)[12]. In this study, four different Mander material models were developed (Table 3).

Table 3. Mander material models

Model Type	Stirrup Diameter	Number of Legs	Stirrup Spacing*	Hook Bend Angle
Model A	8	2/2	200	90°
Model B	8	2/2	100	90°
Model C	8	2/2	200	135°
Model D	8	2/2	100	135°

*Edge regions of reinforced concrete members

Four models with different stirrup configurations (Model A, Model B, Model C, Model D) were analyzed to study the behavior of reinforced concrete elements. Variables such as stirrup spacing (100 mm and 200 mm) and hook bend angles (90° and 135°) were employed to investigate the effect of confinement on the stress-strain behavior of concrete. The stress-strain curves for the models were derived based on the Mander material model. The stress-strain graphs for confined and unconfined concrete elements, as well as the strain values corresponding to damage states for the developed models, are presented below. These results highlight the impact of confinement on the structural performance of the concrete elements.

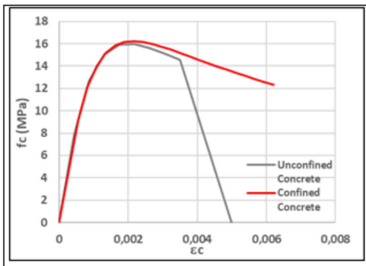

Material	ε_{SH}	ε_{KH}	$\varepsilon_{GÖ}$
Confined Concrete	0,0025	0,0037	0,0049
Longitudinal Reinforcement	0,0075	0,0360	0,0480

Figure 5. Model A mander material model behavior

Model A represents reinforced concrete elements with a stirrup diameter of 8 mm, two-legged stirrups, a spacing of 200 mm, and a hook bend angle of 90°. The wider stirrup spacing and standard hook bend provide limited lateral confinement to the concrete. The stress-strain curve, derived using the Mander material model, indicates moderate strength and ductility. However, the limited confinement reduces the ability to dissipate energy and sustain large deformations under seismic loads. Model A highlights the need for tighter stirrup spacing or improved hook configurations to enhance structural performance (Figure 9).

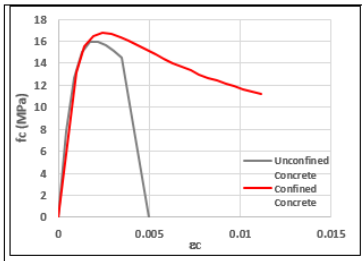

Material	ε_{SH}	ε_{KH}	$\varepsilon_{GÖ}$
Confined Concrete	0,0025	0,0045	0,0060
Longitudinal Reinforcement	0,0075	0,0360	0,0480

Figure 6. Model B mander material model behavior

Model B features a stirrup diameter of 8 mm, two-legged stirrups, a spacing of 100 mm, and a hook bend angle of 90°. The closer stirrup spacing provides a higher level of confinement compared to Model A. The stress-strain curve, derived from the Mander material model, shows enhanced strength and ductility due to the improved lateral support. This configuration allows for better energy dissipation and deformation capacity, making it more effective in seismic conditions. Model B demonstrates the importance of tighter stirrup spacing in improving structural performance(Figure 10).

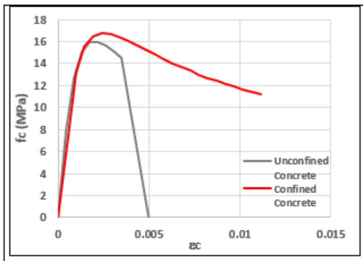

Material	ε_{SH}	ε_{KH}	$\varepsilon_{GÖ}$
Confined Concrete	0,0025	0,0045	0,0060
Longitudinal Reinforcement	0,0075	0,0360	0,0480

Figure 7. Model C mander material model behavior

Model C uses a stirrup diameter of 8 mm, two-legged stirrups, a spacing of 200 mm, and a hook bend of 135°. While the wider stirrup spacing limits the overall confinement, the 135° hook bend improves lateral restraint compared to a 90° bend. The stress-strain curve shows better ductility and strength compared to Model A but lower performance than Model B and Model D. Model C illustrates how an improved hook configuration can partially offset the effects of wider stirrup spacing, resulting in moderate structural performance (Figure 11).

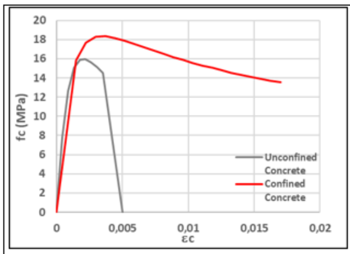

Malzeme	ε_{SH}	ε_{KH}	$\varepsilon_{GÖ}$
Confined Concrete	0,0025	0,0060	0,0081
Longitudinal Reinforcement	0,0075	0,0360	0,0480

Figure 8. Model D mander material model behavior

Model D consists of reinforced concrete elements with a stirrup diameter of 8 mm, two-legged stirrups, a spacing of 100 mm, and a hook bend angle of 135°. This configuration provides the highest level of confinement among the models, combining close stirrup spacing with a superior hook bend angle. The stress-strain curve reveals significant improvements in both strength and ductility, reflecting excellent energy dissipation and deformation capacity under seismic loads. Model D demonstrates the most effective design for maximizing the performance of reinforced concrete elements in high-seismic zones (Figure 12). Previous studies have demonstrated the importance of stirrup configurations and confinement levels in improving the ductility and strength of reinforced concrete elements Sadid and Aydın (2020)[14].

7. Performance evaluations based on mander material models

The performance results of the models were visualized using Python. Different damage states for each model (Limited, Noticeable, Advanced, Collapse) were highlighted with color gradients and presented as a heatmap to facilitate comparative analysis and visual interpretation of the data(Figure 13).

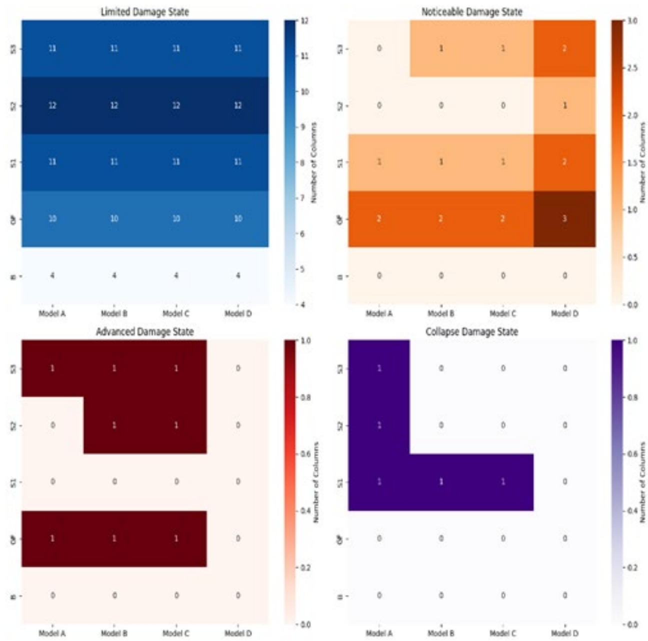

Figure 13. Heatmaps highlighting different damage states

The analyses conducted for the different structural models (Model A, Model B, Model C, and Model D) evaluated the damage states of the columns on each story. For Model A, on the third normal story (3NS), 84.62% (11 columns) were in the limited damage state, while 15.38% (2 columns) were in the noticeable damage state. On the second normal story (2NS), 92.31% (12 columns) experienced limited damage, and 7.69% (1 column) showed noticeable damage. Similarly, on the first normal story (1NS), 84.62% (11 columns) were in the limited damage state, and 15.38% (2 columns) exhibited noticeable damage. On the ground floor (GF), 76.92% (10 columns) were in the limited damage state, and 23.08% (3 columns) showed noticeable damage. In the basement (BM), all columns (100%) exhibited limited damage. For Model B, the results showed that 84.62% of the columns on the 3NS were in the limited damage state, while 15.38% were in the noticeable damage state. On the 2NS, these ratios were 92.31% limited damage and 7.69% noticeable damage. For the 1NS, 84.62% of the columns exhibited limited damage, and 15.38% showed noticeable damage. On the GF, 76.92% of the columns were in the limited damage state, and 23.08% were in the noticeable damage state. In the BM, all columns (100%) were found to have limited damage. Model C displayed similar behavior, with 84.62% limited damage and 15.38% noticeable damage on the 3NS. On the 2NS, 92.31% of the columns exhibited limited damage, while 7.69% showed noticeable damage. On the 1NS, 84.62% of the columns were in the limited damage state, and 15.38% showed noticeable damage. The GF showed higher stress levels compared to other stories, with 76.92% limited damage and 23.08% noticeable damage. In the BM, all columns (100%) remained in the limited damage state. For Model D, 84.62% of the columns on the 3NS exhibited limited damage, and 15.38% showed noticeable damage. On the 2NS, 92.31% of the columns were in the limited damage state, and 7.69% were in the noticeable damage state. On the 1NS, 84.62% of the columns were in the limited damage state, while 15.38% exhibited noticeable damage. On the GF, 76.92% of the columns showed limited damage, and 23.08% showed noticeable damage. In the BM, all columns (100%) were found to be in the limited damage state.

8. Conclusions

In this study, the results of an incremental pushover analysis conducted using the ETABS software for a building located in Samsun were evaluated. The model, created within the framework of the TBDY 2018 code, examined the effects of different stirrup arrangements and hook angles on the building's performance. The analysis revealed that confining the end regions of columns and using 135-degree hook angles instead of 90 degrees significantly improved the damage levels of the columns. Notably, Model D yielded the most favorable results, minimizing the formation of plastic hinges and exhibiting higher ductility at target displacement levels. Conversely, Model A, which lacked confinement and used 90-degree hooks, demonstrated weaker performance due to higher damage levels. In this study, the target displacement values were determined as 57.286 mm in the X-direction and 30.838 mm in the Y-direction. The obtained capacity curves and plastic hinge distributions clearly highlighted the building's seismic performance under various scenarios. The findings emphasize the critical importance of adhering to the design principles outlined in earthquake codes for practical applications. Despite the building being constructed in 1995 according to the 1975 Earthquake Code, it was observed that it did not exhibit collapse or advanced damage levels when analyzed under TBDY 2018 standards, provided that the code's specifications were followed. This underscores the necessity of considering regulatory requirements and accurately implementing material properties and detailing during the design phase to ensure seismic resilience. Future research could focus on various aspects to gain a deeper understanding of seismic performance and address existing gaps. Specifically, nonlinear time-history analyses should be conducted, and the results compared with pushover analysis findings to provide a more realistic understanding of structural behavior. The effects of material variables such as concrete strength, steel quality, and confinement reinforcement ratios should be thoroughly investigated to clarify their roles in structural performance. For retrofitting older buildings, the effectiveness of modern techniques such as FRP wrapping and the addition of shear walls should be explored, with an emphasis on their contributions to seismic resilience. Furthermore, comprehensive studies on structural irregularities (both vertical and horizontal) should evaluate their impact on plastic hinge formation and overall performance. To enhance the reliability of numerical analyses, experimental studies on reinforced concrete elements with varying stirrup configurations should be conducted to validate model predictions. These efforts will provide scientific and practical solutions to improve seismic resilience and make significant contributions to design and retrofitting processes.

Nomenclature

DD-2 : Design basis earthquake
Ss : Short Period Spectral Acceleration Coefficient
S1 : 1-Second Period Spectral Acceleration Coefficient
ZC : Soil class
Sa : Spectral acceleration
Sd : Spectral displacement

Declaration of Conflict of Interests

The authors declare that there is no conflict of interest. They have no known competing financial interests or personal relationships that could have appeared to influence the work reported in this paper.

References

[1.] AFAD. Turkey Earthquake Hazard Map. https://tdth.afad.gov.tr

[2.] Republic of Turkey Ministry of Public Works and Settlement. Regulation on Structures to be Built in Disaster Areas. Official Gazette 11 July 1975 (1975) 15257.

[3.] DBYBHY. Regulation on Buildings to be Constructed in Earthquake Zones. Ministry of Environment and Urbanization, Ankara (2007).

[4.] TBDY. Turkey Building Earthquake Code. Ministry of Environment and Urbanization, Ankara (2018).

[5.] Yüzbaşı, J., Yerli, H.R.. Performance analysis and strengthening of reinforced concrete structures under seismic effects. Çukurova University Journal of Engineering and Architecture Faculty 33(2018)273-286.

[6.] Döndüren, M.S., Şeyda, H.A.V.A., Ecemiş, A.S.. Analysis of a reinforced concrete building using the equivalent earthquake load method according to DBYBHY 2007 and TBDY 2018 regulations. Konya Journal of Engineering Sciences 9(2021)507–521.

[7.] Demir, A., Kayhan, A.H.. Comparison of time-history analysis results in compliance with the 2007 Earthquake Code and Turkey Building Earthquake Code. 4th International Earthquake Engineering and Seismology Conference, Anadolu University, Eskişehir (2017).

[8.] Kanamori, H., Brodsky, E.E.. The physics of earthquakes. Reports on Progress in Physics 67(2004)1429.

[9.] Bozkurt, E.. Neotectonics of Turkey – a synthesis. Geodinamica Acta 14(2001)3-30.

[10.] Barka, A.A., Kadinsky-Cade, K.. Strike-slip fault geometry in Turkey and its influence on earthquake activity. Tectonics 7(1988)663-684.

[11.] FEMA. Prestandard and Commentary for the Seismic Rehabilitation of Buildings. Federal Emergency Management Agency (2000).

[12.] Mander, J.B., Priestley, M.J.N., Park, R.. Theoretical stress-strain model for confined concrete. Journal of Structural Engineering 114(1988)1804–1826.

[13.] Demirel, Y., Polat, Ö.. Examination of experimental and theoretical behavior of a reinforced concrete room under internal explosion loads. Journal of Civil Engineering Beyond Limits 1(2020)60-75.

[14.] Sadid, A.J., Aydın, A.C.. Simulation of cold-formed steel shear wall sheathed with steel plate: Non-linear finite element modelling and analysis. Journal of Civil Engineering Beyond Limits 2(2020)30-42.

[15.] Özmen, H.B., İnsel, M., Bilgin, H.. The effect of confined concrete behavior on the performance of reinforced concrete elements and systems. Gazi University Journal of Engineering and Architecture Faculty 22(2007)375-383.

[16.] Çavdar, Ö., Bayraktar, A.. Pushover and nonlinear time history analysis evaluation of a RC building collapsed during the Van (Turkey) earthquake on October 23, 2011. Natural Hazards 70(2014)657-673.

[17.] Özkarabulut, A.. Performance analysis of reinforced concrete plane frames using different modeling approaches. Master's Thesis, Çanakkale Onsekiz Mart University, Graduate School of Science, Department of Civil Engineering, Çanakkale (2024).

[18.] ETABS. Integrated Software for Structural Analysis and Design. Computers and Structures, Inc., California (2024).

How to Cite This Article

Kırat, M. and Yılmaz, M.F., Seismic Evaluation of RC Building Designed by 1975 Turkish Seismic Code (A Case Study), Civil Engineering Beyond Limits, 3(2024), 1964.
https://doi.org/10.36937/cebel.2024. 1964.